Constitutive Behavior of Salina Salt from the Cleveland Mine

K. D. Mellegard, T. W. Pfeifle and P. E. Senseny
RE/SPEC Inc.,
Rapid City, South Dakota, USA

ABSTRACT

A suite of triaxial compression experiments was completed on 100-mm-diameter specimens of salt taken from the Cleveland Salt Mine in Cleveland, Ohio. This paper presents the apparatus and procedures used to generate and evaluate the triaxial data obtained from Cleveland salt. Various stress and temperature conditions were imposed to allow construction of an exponential-time constitutive law that can model arbitrary thermomechanical histories. Predicted and measured curves are presented to illustrate how well the derived law can reproduce the data.

INTRODUCTION

In 1982 an in situ experiment was being proposed at the Whiskey Island Salt Mine in Cleveland, Ohio under the auspices of the U.S. National Waste Terminal Storage (NWTS) Program. To design a test plan for that experiment, the geologic media at the site had to be characterized. This paper presents part of the characterization effort; namely, the development of a constitutive law to describe the time-dependent deformation of salt at the Whiskey Island Salt Mine.

The constitutive law includes both elastic and inelastic components. The elastic component combines Hooke's law and linear thermal expansion while the inelastic component is based on a generalization of a law used to describe constant-stress (creep) data. The elastic parameters may be determined from constant-stress-rate experiments and constant-temperature-rate experiments. The inelastic parameters are determined by fitting creep experiment data to an exponential-time creep law:

$$\epsilon_c = \dot{\epsilon}_{ss}t + e_a\{1 - \exp(-\xi t)\} \quad (1)$$

where ϵ_c is creep strain, t is time and $\dot{\epsilon}_{ss}$, e_a and ξ are regression coefficients to be determined for each experiment. In general, these three parameters depend on stress and temperature. This type of creep law is based on first-order kinetics and was first evaluated for southeastern New Mexico bedded salt (Herrmann *et al.*, 1980). It has since been identified as the baseline creep law to be used in the NWTS Program (Senseny, 1983) and was evaluated for salt from the dome at Avery Island, LA (Mellegard and Senseny, 1983).

CREEP LAW CHARACTERISTICS

The creep rate of salt may be described using first-order kinetics (Herrmann et al, 1980)

$$\frac{d\dot{\epsilon}}{dt} = -\xi(\dot{\epsilon} - \dot{\epsilon}_{ss}) \quad (2)$$

where:

$\dot{\epsilon}$ = Current Creep Rate
$\dot{\epsilon}_{ss}$ = Steady State Creep Rate
ξ = Relaxation Frequency.

Integration of Equation 2 twice with respect to time leads to the expression for creep strain

$$\epsilon_c = \dot{\epsilon}_{ss}t + e_a\{1 - \exp(-\xi t)\} \quad (3)$$

where:

ϵ_c = Creep Strain
e_a = Asymptotic Transient Strain

and the other terms were defined previously. Models for both transient and steady-state creep strain are described by Equation 3.

The form of the exponential-time law given by Equation 3 relates a scalar measure of creep strain at constant stress and temperature to time. However, to use this law for analysis of structures in salt, it must be written in a form that relates components of the inelastic strain rate tensor to components of the stress tensor for arbitrary thermomechanical history. When the appropriate stress and temperature dependence of the parameters $\dot{\epsilon}_{ss}$, e_a and ξ are introduced, and the elastic component is included, the exponential-time law may be written as (Senseny, 1983):

$$\dot{\epsilon}_{ij} = \frac{1}{E}\left[(1+\nu)\dot{\sigma}_{ij} - \nu\,\dot{\sigma}_{kk}\delta_{ij}\right] + \beta\dot{T}\delta_{ij}$$

$$+ A(3J_2')^{\frac{n+1}{2}} \exp(-Q/RT)$$

$$\times \left\{ 1 + B\,\epsilon_a - \frac{B\epsilon_a\,\xi}{(J_2')^{n/2}\exp(-Q/RT)} \right.$$

$$\times \int_0^t (J_2')^{n/2} \exp(-Q/RT)$$

$$\left. \times \exp\left[-\int_{t''}^{t} \xi\, dt' \right] dt'' \right\} \frac{\sigma_{ij}'}{2J_2'}$$

$$\xi = \begin{cases} BA(3J_2')^{n/2}\exp(-Q/RT) & \dot{\epsilon}_{ss} \geq \dot{\epsilon}_{ss}^* \\ B\dot{\epsilon}_{ss}^* & \dot{\epsilon}_{ss} \leq \dot{\epsilon}_{ss}^*. \end{cases} \quad (4)$$

where:

- $\dot{\epsilon}_{ij}$ is the total strain rate
- $\dot{\sigma}_{ij}$ is the stress rate
- σ_{ij}' is the stress deviator
- δ_{ij} is the Kronecker delta
- J_2' is the second invariant of the stress deviator
- T is the absolute temperature
- β is the coefficient of linear thermal expansion
- E, ν are Young's modulus and Poisson's ratio, determined from the unload-reload portion of the constant-stress rate tests
- A, n, Q/R, B, ϵ_a, $\dot{\epsilon}_{ss}^*$ are parameters whose values are determined by regression analysis of data from creep tests.

The parameter Q/R is usually interpreted as the ratio of the activation energy of the rate-controlling deformation mechanism to the universal gas constant. The parameter ϵ_a is the asymptotic transient strain. The parameter $\dot{\epsilon}_{ss}^*$ is the critical steady-state strain rate criteria used to differentiate between the two regimes of the relaxation parameter, ξ.

To evaluate the six inelastic parameters that appear in Equation 4, each creep experiment is fitted with Equation 3 to get regression values for $\dot{\epsilon}_{ss}$, e_a, and ξ. Establishing the stress and temperature dependence of these three regression parameters gives values for the six inelastic parameters. The complete procedure for evaluating all the parameters except β is presented in detail later in this paper. The thermal expansion coefficient, β, was not determined experimentally. A value of $41 \times 10^{-6}\ K^{-1}$ may be used (Bradshaw and McClain, 1971).

TESTING MACHINES

All the triaxial compression experiments on salt were conducted on four machines designed by Dr. W. R. Wawersik of Sandia National Laboratories. These four machines have been described previously (Mellegard *et al.*, 1981) and have the distinctive capability of measuring volumetric changes during a triaxial compression test. The volumetric measurements allow calculation of average lateral strain.

A typical machine load frame schematic with prominent components labeled for reference is presented in Figure 1. The machines use a single-ended triaxial pressure vessel that accommodates a cylindrical specimen of 100-mm diameter with a length-to-diameter ratio of L:D = 2. A hydraulic cylinder bolted to the base of the load frame drives the loading piston which applies axial compressive force to the specimen. Confining pressure is applied to the jacketed specimen by pressurizing the sealed vessel chamber with silicone oil. A dilatometer system maintains constant confining pressure and provides the volumetric measurement for making lateral strain calculations.

The testing machines can apply compressive axial stresses

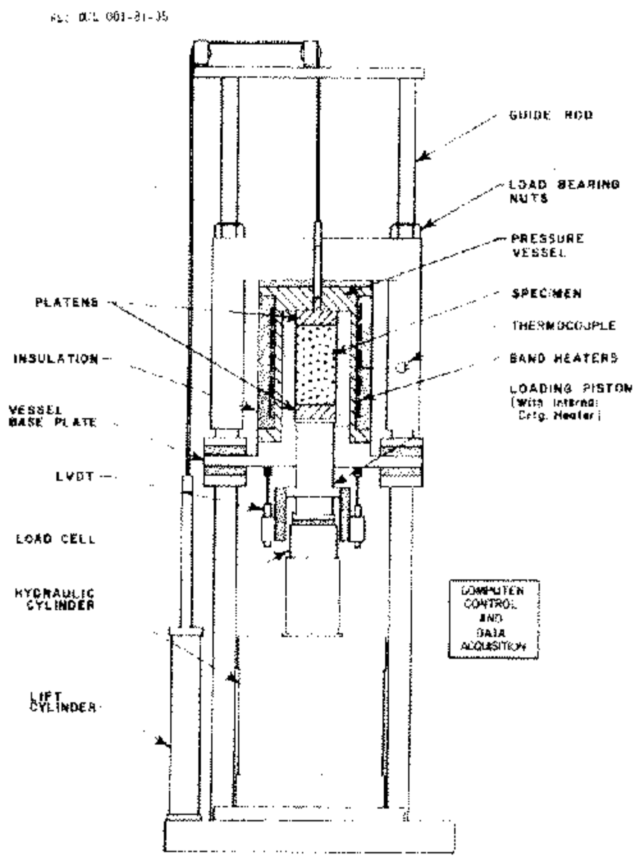

Figure 1. Test Machine Schematic.

up to 200 MPa and confining pressures up to 70 MPa. The heating system can maintain constant test temperatures within ±1°C up to 200°C.

Data collected during each test are time, temperature, axial stress, confining pressure, axial displacement and volumetric displacement. A microcomputer logs data at selected intervals of time and strain and converts the transducer signals to engineering units.

Axial stress data are provided by an external load cell. Back-up readings are available from a mechanical gage connected directly into the hydraulic pressure system.

A pressure transducer instrumented with strain gauges connected to the triaxial pressure vessel provides confining pressure data. This transducer also provides the feedback signal required by the dilatometer for constant pressure control.

Two Linear Variable Differential Transformers (LVDT) provide indirect axial displacement data by measuring piston displacement relative to the baseplate of the vessel. During data reduction, calibration factors remove the machine softness component of the indirect reading to give actual specimen displacements.

Volumetric displacement data (lateral strain) are provided by a rotary potentiometer mounted on the intensifier shaft of the dilatometer.

Temperature data are collected from a thermocouple mounted in the wall of the triaxial test vessel. This thermocouple also provides the feedback signal for constant temperature control.

The transducers used to collect data were calibrated against standards traceable to the National Bureau of Standards (NBS). Accuracies and resolutions determined for each type of measurement system are presented in Table 1.

SPECIMENS

The specimens were right circular cylinders subcored from 200-mm-diameter cores taken from the 538-m (1765-foot) level of the mine. The specimens were nominally 100 mm in diameter and 200 mm in length after subcoring. Subsequently, the specimen ends were machined flat and parallel to within 0.02 mm, using a lathe equipped with carbide tooling.

The specimens were composed primarily of salt but were not homogeneous. The specimens usually contained at least two thick bands of anhydrite lying parallel to the horizontal axes of the specimens. These anhydrite bands ranged from 3 mm to 30 mm in thickness and were usually located near the quarter points of the vertical axis.

TABLE 1

Calibration Results

Measurement System	Working Range	Accuracy	Resolution
Axial Strain (Percent)	0–12.5	0.006	0.001
Lateral Strain (Percent)	0–8	0.004	0.002
Axial Stress (MPa)	0–70	0.2	0.007
Confining Pressure (MPa)	0–15	0.035	0.007
Temperature (°C)	20–200	2.0	0.1

TEST PROCEDURE

When conducting a triaxial compression creep test, a hydrostatic stress is initially applied to the specimen, and the dilatometer servosystem is actuated to maintain constant pressure. The system is then allowed to stabilize prior to application of axial stress difference. Tests run at elevated temperatures are heated to the desired temperature before the confining pressure is applied. After equilibration under hydrostatic conditions, axial stress difference is applied as quickly as possible (<30 seconds); time and strain are reset to zero; and the creep test begins.

A constant axial stress is maintained on the specimen by a nitrogen-charged bladder accumulator. The axial stress difference is maintained as the specimen deforms by increasing the axial load periodically. Assuming the deformed specimen maintains the shape of a right circular cylinder, the equation for the correction for change of cross-sectional area is:

$$A_R = A_o\left(1 + \frac{D_R - D_o}{D_o}\right)^2 \tag{5}$$

where:

A_R = Current area of the specimen;
A_o = Original area of the specimen;
D_R = Current specimen diameter; and
D_o = Original specimen diameter.

A set of regression parameter values ($\dot{\epsilon}_{ss}$, e_a, ξ) are calculated for each creep test using Equation 3. The values determined for those regression parameters will be incorrect if the creep test duration is too short. The appropriate test duration varies but can easily exceed three months. The regression parameters approach their final values as the creep test progresses, as is demonstrated in Figure 2. The ordinate scale represents normalized parameter values based on final asymptotic values. The abscissa scale represents actual creep time. Construction of Figure 2 was accomplished by first fitting to the entire data set and then fitting to successively shorter duration subsets of the data. Approximately 100 data points are generated this way. This procedure is carried out periodically during the term of the creep test and the test is allowed to continue until a plot similar to Figure 2 appears.

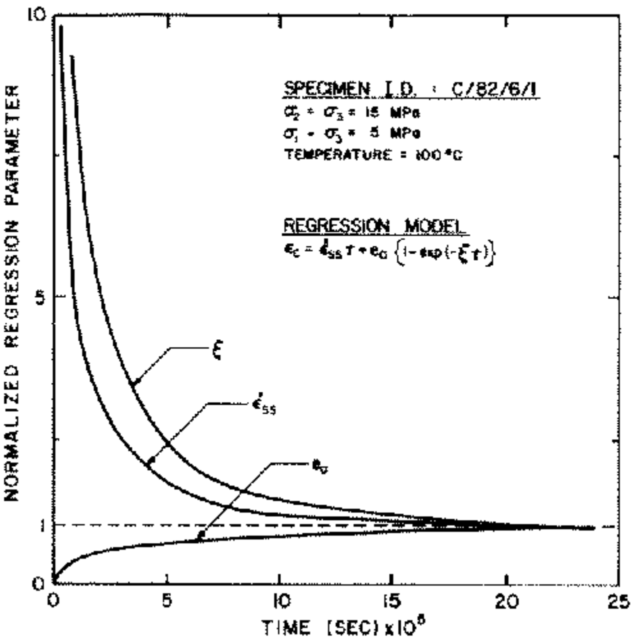

Figure 2. Regression Parameters as a Function of Creep Test Duration.

TEST RESULTS

Parameters to fit Equation 1 to each of the creep tests were calculated by using a routine that provides least square estimates for non-linear functions. The tests are listed in Table 2 along with test conditions and regression values. The data in Table 2 may be used to determine the stress and temperature dependence of each of the three regression parameters.

The first step in determining the inelastic parameters is a determination of how the steady-state rates depended on stress and temperature. The expression

$$\dot{\epsilon}_{ss} = A\,\sigma^{n} \exp(-Q/RT) \qquad (6)$$

where:

σ = Axial Stress Difference
T = Absolute Temperature

was fitted to the data in Table 2 using a non-linear least squares routine to determine the inelastic parameters A, n, and Q/R, and their standard errors. The parameter Q/R is usually interpreted as the ratio of the activation energy of the rate-controlling deformation mechanism to the universal gas constant. The fitted equation is

$$\dot{\epsilon}_{ss} = 8.57 \times 10^{-3}\,\sigma^{4.08} \exp(-8685/T) \qquad (7)$$

where the units on stress and temperature are MPa and Kelvin, respectively. In the worst case, the difference between predicted and measured strain rate results in a 74 percent error. Some of this variability may result from the anhydrite bands in the specimens.

For constant stress and temperature (creep), the constitutive law presented in Equation 4 may be written

$$\epsilon_c = \begin{cases} \dot{\epsilon}_{ss}\{t + \epsilon_a/\dot{\epsilon}^*_{ss}[1 - \exp(-B\dot{\epsilon}^*_{ss}t)]\} & \text{for } \dot{\epsilon}_{ss} \leq \dot{\epsilon}^*_{ss} \\ \dot{\epsilon}_{ss}t + \epsilon_a[1 - \exp(-B\dot{\epsilon}_{ss}t)] & \text{for } \dot{\epsilon}_{ss} \geq \dot{\epsilon}^*_{ss}. \end{cases} \qquad (8)$$

The creep law parameters ϵ_a, B and $\dot{\epsilon}^*_{ss}$ may be found by determining the stress and temperature dependence of the regression parameters e_a and ξ presented in Table 2.

The stress and temperature dependence of the regression parameters e_a and ξ is different at high steady strain rates than at low steady strain rates (Herrmann *et al.*, 1980). The two regions are divided by the critical steady strain rate, $\dot{\epsilon}^*_{ss}$. For steady strain rates above $\dot{\epsilon}^*_{ss}$, the creep law parameters B and ϵ_a are given by $B = \xi/\dot{\epsilon}_{ss}$ and $\epsilon_a = e_a$. For steady strain rates below $\dot{\epsilon}^*_{ss}$, $B = \xi/\dot{\epsilon}^*_{ss}$ and $\epsilon_a = (\dot{\epsilon}^*_{ss}/\dot{\epsilon}_{ss})\,e_a$. A non-linear least squares routine was used to simultaneously determine the three creep law parameters $\dot{\epsilon}^*_{ss} = 3.17 \times 10^{-9}\,s^{-1}$, B = 80 and $\epsilon_a = 0.028$. Substitu-

TABLE 2

Summary of Creep Tests Initiated on Cleveland Salt

Specimen I.D.	Stress* (MPa)	Temp. (°C)	Duration (Days)	Regression Parameters		
				$\dot{\epsilon}_{ss}$	e_a	ξ
C/82/20/1	15	25	107	1.137×10^{-10}	3.960×10^{-3}	5.546×10^{-6}
C/82/8/1	10	50	19	2.215×10^{-10}	6.266×10^{-4}	1.639×10^{-5}
C/82/18/1	15	75	156	5.471×10^{-9}	2.221×10^{-2}	9.359×10^{-7}
C/82/6/1	5	100	28	1.843×10^{-9}	1.756×10^{-3}	1.940×10^{-5}
C/82/7/1	10	100	28	1.254×10^{-8}	8.644×10^{-4}	2.081×10^{-4}
C/82/9/1	15	100	22	5.699×10^{-8}	3.224×10^{-2}	3.904×10^{-6}
C/82/10/1	7.5	100	130	2.952×10^{-9}	6.524×10^{-3}	2.365×10^{-7}
C/82/2/1	5	200	25	4.641×10^{-8}	4.162×10^{-2}	3.810×10^{-6}
C/82/14/1	10	200	<1	3.336×10^{-6}	1.959×10^{-2}	1.015×10^{-2}
C/82/12/1	7.5	200	3	3.780×10^{-7}	3.494×10^{-2}	2.734×10^{-5}

*—Axial Stress Difference. Confining pressure was 15 MPa for all tests.

tion into Equation 8 provides the following creep model for the Cleveland salt experiments in Table 2:

for $\dot{\epsilon}_{ss} \le \dot{\epsilon}^*_{ss} = 8.57(10^{-9})\ s^{-1}$

$$\epsilon_c = 8.57(10^{-3})\,\sigma^{4.08}\exp(-8685/T)\{t + 8.84(10^6)[1 - \exp\{-2.53(10^{-7})t\}]\} \qquad (9)$$

and

for $\dot{\epsilon}_{ss} \ge \dot{\epsilon}^*_{ss}$

$$\epsilon_c = 8.57(10^{-3})\,\sigma^{4.08}\exp(-8685/T)\,t + 0.028[1 - \exp\{-0.69\,\sigma^{4.08}\exp(-8685/T)\,t\}] \qquad (10)$$

where the units on σ, T, and t are MPa, K and s, respectively.

The quality of the reproduction of the creep data, based on Equations 9 and 10, for various stress levels at temperatures of 100°C and 200°C, respectively, are illustrated in Figures 3 and 4. The maximum difference between calculated and measured strains occurs at a stress difference of 15 MPa at 100°C and represents approximately 30 percent error in prediction.

At this point, the six regression parameters needed to model the creep deformation of salt at constant stress have been determined. The two remaining terms in Equation 4 yet to be determined are the elastic parameters E and ν. These parameters are evaluated from unload/reload cycles in constant-stress-rate triaxial compression tests. Two tests were performed at 25°C; the first at a confining pressure of 1 MPa and the second at 5 MPa. The stress rate in both experiments was .025 MPa/sec. The values of E and ν obtained at pressures of 1 MPa and 5 MPa were {24.9 GPa, 0.27} and {28.0 GPa, 0.27}, respectively. The average values then are E = 26.5 GPa and ν = 0.27. These values are comparable to the average values of E = 30 GPa and ν = 0.35 determined for ten different salts in the United States (Hansen *et al.*, 1984).

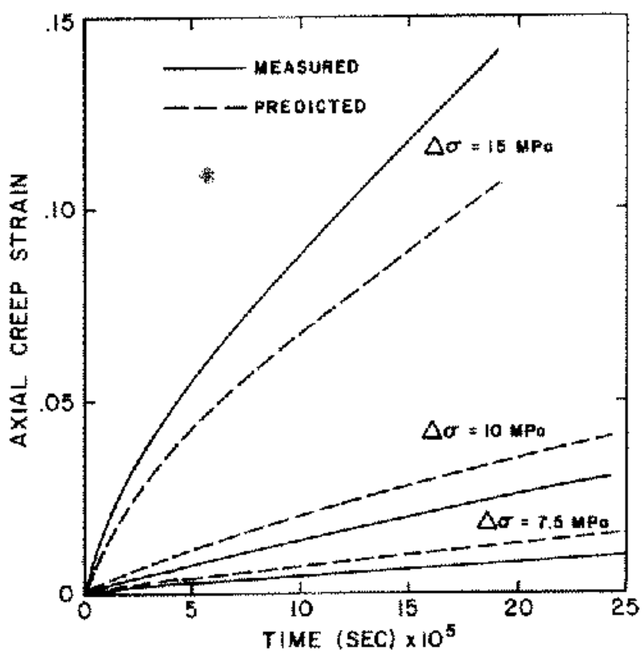

Figure 3. Measured and Predicted Axial Creep Strain as a Function of Time at 100°C.

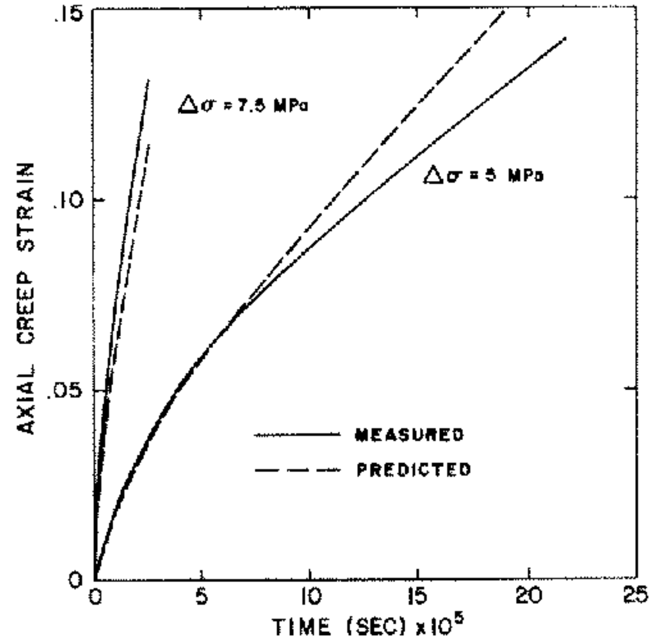

Figure 4. Measured and Predicted Axial Creep Strain as a Function of Time at 200°C.

All nine of the parameters required by Equation 4 are summarized in Table 3.

CONCLUSION

A series of triaxial compression experiments were conducted on Cleveland salt specimens to generate creep and stress rate data. The creep data results were used to determine six parameters in an exponential-time creep law. The stress rate data provided values of Young's modulus and

TABLE 3

Creep Law Parameters Determined For Cleveland Salt

Parameter	Value ± Std. Error	Units
A	$(8.57 \pm 8.72) \times 10^{-3}$	MPa^{-n}
n	4.08 ± 0.64	
Q/R	8685 ± 641	K
$\dot{\epsilon}^*_{ss}$	$(3.17 \pm 2.46) \times 10^{-9}$	s^{-1}
ϵ_a	$.028 \pm .032$	
B	80 ± 17	
E	26.4 ± 2.4	GPa
ν	0.27 ± 0.01	
β	$(41 \pm 3) \times 10^{-6}$	K^{-1}

Poisson's ratio. These eight values are used in a tensorial rate form of a constitutive relationship that can be used to model deformation of underground openings in salt.

The law was used to predict the data from which it was constructed. The transient creep regimes were not always very well predicted. The predicted steady-state strain rates varied by a factor of four in the worst case. Much of the variation may be caused by the thick anhydrite bands in the specimens.

REFERENCES

Bradshaw, R. L., and W. C. McClain, eds. 1981. "Project Salt Vault: A Demonstration of the Disposal of High Activity Solidified Wastes in Underground Salt Mines," *ORNL-4555*, Oak Ridge National Laboratory, Oak Ridge, TN.

Hansen, F. D., K. D. Mellegard and P. E. Senseny. 1984. "Elasticity and Strength of Ten Natural Rock Salts," To appear in the Proceedings of the First Conference of the Mechanical Properties of Salt, H. R. Hardy, ed.

Herrmann, W., W. R. Wawersik and H. S. Lauson. 1980. "A Model for Transient Creep of Southeastern New Mexico Rock Salt," Sandia National Laboratories, Albuquerque, NM, *SAND-80-2172*, Prepared by Sandia National Laboratories under Contract DE-AC04-76DP00789 with the United States Department of Energy.

Mellegard, K. D. and P. E. Senseny. 1983. "Exponential-Time Creep Law for Avery Island Salt," Prepared by RE/SPEC Inc., Rapid City, SD, RSI-0164, for Office of Nuclear Waste Isolation, Battelle Memorial Institute, Columbus, OH, *ONWI*-329.

Mellegard, K. D., P. E. Senseny and F. D. Hansen. 1981. "Quasi-Static Strength and Creep Characteristics of 100-mm-Diameter Specimens of Salt From Avery Island, Louisiana," Prepared by RE/SPEC Inc., Rapid City, SD, RSI-0140, for Office of Nuclear Waste Isolation, Battelle Memorial Institute, Columbus, OH, *ONWI-250*.

Senseny, P. E. 1983. "Review of Constitutive Laws Used to Describe the Creep of Salt," Prepared by RE/SPEC Inc., Rapid City, SD, RSI-0151, for Office of Nuclear Waste Isolation, Battelle Memorial Institute, Columbus, OH, *ONWI-295*.